RB5: A Low-Cost Wheeled Robot for Real-Time Autonomous Large-Scale Exploration

Adam Seewald[1], Marvin Chancán[1], Connor M. McCann[2], Seonghoon Noh[1], Omeed Fallahi[1], Hector Castillo[1], Ian Abraham[1], and Aaron M. Dollar[1]

***Abstract*—**

***Index Terms*—Article submission, IEEE, IEEEtran, journal, LATEX, paper, template, typesetting.**

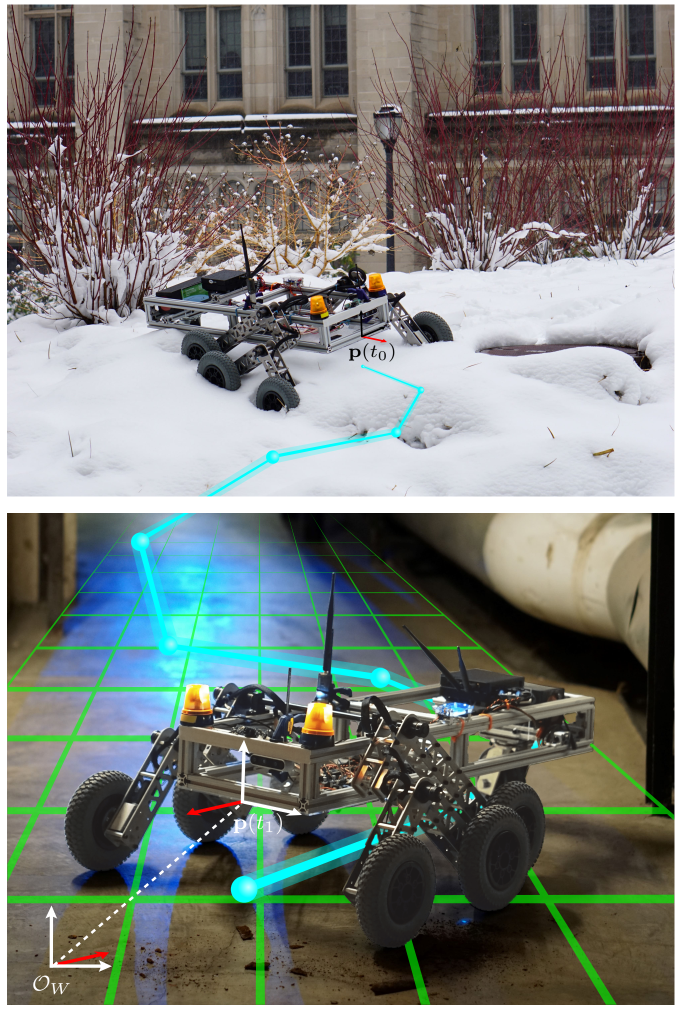

Fig. 1: . . . .

I. Introduction

WIDELY used in cluttered environments [1]–[4], mobile robots can both substitute [5] and outperform humans in, e.g., areas that are too far or too dangerous to navigate [6]–[9]. In these areas, robots are often required to identify their surroundings by sensing the environment [10] and planning and executing complex trajectories [11], [12]. With little or no human intervention [13], this problem is known in the literature as autonomous exploration [11]. While successful in challenging indoor and outdoor environments [14], [15], autonomous exploration is especially useful in dynamic environments with no prior knowledge of the space to be covered [5], [16]. Despite recent advancements, autonomy is limited and costly in such environments. Many approaches that tackle autonomous exploration integrate commercial robots with sensing equipment that is both prohibitively expensive and difficult to maintain [8], [9], [14], [15], [17]–[20]. There is a wide range of methodologies for autonomous exploration at present [15], [21] nonetheless, which span from algorithmic foundations [15], [19], [22] to system-of-systems frameworks where, e.g., a multitude of robots integrate existing algorithms with sensors for large-scale exploration [3], [7]–[9], [18]. Recent efforts in this direction include low-cost robots for exploration [17], [23], [24] but lack terrain adaptability [17] and computational capabilities [23], [24] often required to navigate outdoors in the real-world [2], [5].

Furthermore, in areas that are ambiguous or challenging to traverse–albeit autonomous–state-of-the-art approaches rely on humans for supervision and high-level decision-making [3], [7], [8]. As a result, robots often operate close to humans or require expensive network equipment, such as a mesh of communication devices [2], [3], [9], or existing network infrastructure [25]–[27], thereby restricting autonomous exploration to indoor settings only [12], [28]–[31]. Conversely, our methodology exploits LoRa–an inexpensive long-range and low-power communication technology [32] from the internet-of-things domain–with a customized communication protocol for human intervention in, e.g., the eventuality of the robot being unable to move with the local sensory information.

Starting from the cost advantages of LoRa communication, we develop here RB5–a novel rocker-bogie-like mobile robot capable of exploring autonomously dynamic indoor and outdoor environments–and an open-source robot operating

Manuscript received: Month, Day, Year; Revised Month, Day, Year; Accepted Month, Day, Year.

This paper was recommended for publication by Editor Editor A. Name upon evaluation of the Associate Editor and Reviewers' comments.

[1]A. S., C. M., S. N., O. F., H. C, I. A., and A. M. D. are with the Department of Mechanical Engineering and Materials Science, Yale University, CT, USA. Email: adam.seewald@yale.edu;

C. M. C. is with the School of Engineering and Applied Sciences, Harvard University, MA, USA.

Digital Object Identifier (DOI): see top of this page.

system (ROS)-based [33] exploration framework. Rocker-bogie mobile robots comprise a multi-body system with a moving base [24], [34], [35] (see Figure 1) and provide rough terrain static adaptability [36]. They are cheaper than, e.g., legged robots in terms of cost per unit and operation, as they are able to overcome obstacles without costly computations for gait adaptation and planning [17]. Hardware-wise, RB5 maintains a lower sensory footprint with low-cost components, whereas software-wise, it integrates multiple modules into the exploration framework. Being able to operate in both unknown and GPS-denied environments, RB5 derives its position using a state-of-the-art simultaneous localization and mapping (SLAM) algorithm [37], and the trajectory with a novel methodology that extends exploration literature with a path following vector field [38] from the aerial robotics domain [39]–[41]. This allows RB5 to explore its surroundings at lower frequencies, utilizing cheaper computing hardware compared to state-of-the-art approaches [8], [9], [15], [19].

The remainder of the letter is structured as follows. In Section V data show improved "coverage per cost" over the baseline of existing autonomous exploration system-of-systems with indoor and outdoor "in the field" experiments. Secs. IV describe RB5 from the hardware and software standpoints. Sec. II summarizes and compares existing literature, Sec. III formalizes the problem of autonomous exploration, and Sec. VI drafts conclusions and future directions.

II. Related Work

III. Problem Formulation

The problem considered in this work to showcase RB5 for large-scale exploration is that of exploring a bounded volume $\mathcal{Q} \subseteq \mathbb{R}^3$ with respect to an inertial navigation frame $\mathcal{O}_W$. If the notation $[n]$ denotes a set with positive naturals up to n and $[n]_{>0}$ with strictly positive naturals, we are interested in collision-free trajectories that explore $\mathcal{Q}$ and avoid $i \in [n]_{>0}, n \in \mathbb{N}_{\geq 0}$ obstacles $\mathcal{Q}^{O_i} \subset \mathbb{R}^3$. We can approximate the space that delimits $\mathcal{Q}$ and $\mathcal{Q}^{O_i}$ for each i with a set of vertices within which the two sets are contained.

Problem (Exploration)**.** Consider sets of vertices $V := \{\mathbf{v}_1, \mathbf{v}_2, \dots\}$, $O_i := \{\mathbf{o}_{i,1}, \mathbf{o}_{i,2}, \dots\}$ with $i \in [n], \mathbf{v}_j, \mathbf{o}_{i,k} \in \mathbb{R}^2$, $\forall j \in [|v|]$, $k \in [|o_i|]$ a point w.r.t. $\mathcal{O}_W$. Let V enclose $\mathcal{Q}$, O_i $\mathcal{Q}^{O_i}$ per each i. The *exploration problem* is the problem of finding the coverage that visits each point $\mathbf{p} \in \mathcal{Q} \cap \mathcal{Q}^{O_1} \cap \mathcal{Q}^{O_2} \cap \dots \cap \mathcal{Q}^{O_n} := \mathcal{Q}^V$.

Here the notation $|\cdot|$ denotes the cardinality and $\mathbb{R}$, $\mathbb{Z}$ are reals and integers. Bold notation is used for vectors.

Let ϕ be a path function, i.e., a function RB5 tracks as it explores its surroundings in $\mathcal{Q}^V$, avoiding the obstacles $\mathcal{Q}^{O_i}$.

Definition III.1 (Path function)**.** $\phi : \mathbb{R}^2 \to \mathbb{R}$ is a two-dimensional continuous and differentiable *path function* of the x, y components of $\mathbf{p}$.

Definition III.2 (Coverage)**.** Given a tuple with a path function and its time component, $\langle \phi, t \rangle$, the *coverage* is the collection of multiple tuples.

The large-scale exploration framework (see Sec. IV-B) derives ϕ at each sampling step and adds it to the global "coverage stack". The process ends once $\mathcal{Q}^V$ is covered.

IV. Methods

The methods section justifies design and implementation choices for the RB5 robot in terms of both the low-cost hardware design and the software implementation for autonomous large-scale exploration in respectively Sec. IV-A and IV-B.

A. Low-cost hardware design

The RB5 mobile robot adopts a rocker-bogie suspension system [42] found on NASA's rovers including Sojourner and Curiosity. On either side of the robot, an upside-down V-shaped linkage called the rocker pivots about an axis on the robot frame. The rocker has a wheel at one end and a smaller V-shaped linkage on the other arm. The smaller linkage, called the bogie, can pivot about an axis on the rocker and has two wheels at its tips. The articulated nature of the rocker-bogie suspension allows the mobile robot to adapt to uneven terrains [24], [35], [36] as the rocker and bogie pivot to maintain wheel contact [35]. Each of the six wheels in the rocker-bogie suspension is actuated by a DC gear motor, whereas the rotational degrees of freedom in the rocker-bogie suspensions are passive. Since the wheels are all parallel and cannot rotate out of the plane, the robot uses the same actuation strategy as that of a differential drive vehicle to move straight and make turns by controlling the left and right sets of wheels in the same and opposite directions. Given that RB5 has multiple wheels on each side, its ability to make turns is reduced compared to a differential drive vehicle. Due to its extended body length, RB5 incorporates a caster wheel in the back to support the rear end of the frame.

The robot frame's dimensions are 914 by 330 millimeters, and the robot's bounding box dimensions are 991 by 762 mm. The frame consists of one inch aluminum extrusions and acrylic sheets, and the rocker and bogie linkages are assembled from aluminum sheets and standoffs. The pivots of the bogie and rocker sit at 240 and 330 mm from the ground respectively, providing a clearance of approximately 190 mm beneath the robot frame. The two wheels on each bogie linkage are coplanar, but the wheel on the corresponding rocker linkage is closer to the medial plane of the robot. Motor control is performed by a Teensy (R) 4.0 microcontroller board sending PWM commands to six DRV8871 motor driver boards. An onboard 24 volts $LiFePO_4$ battery provides power for the logic boards and motor drives.

B. Autonomous large-scale exploration

There is a large body of work for robot exploration [15], [19], [21], [22], [43]. While the majority exploits the concept of frontiers [44], i.e., boundaries between known and unknown space, mixed approaches are emerging [15], [45], [46]. Especially useful in the presence of diverse sensing modalities, e.g., involving raw sensory data, topologies, semantics, etc., they have multiple advantages for real-world environments [15],

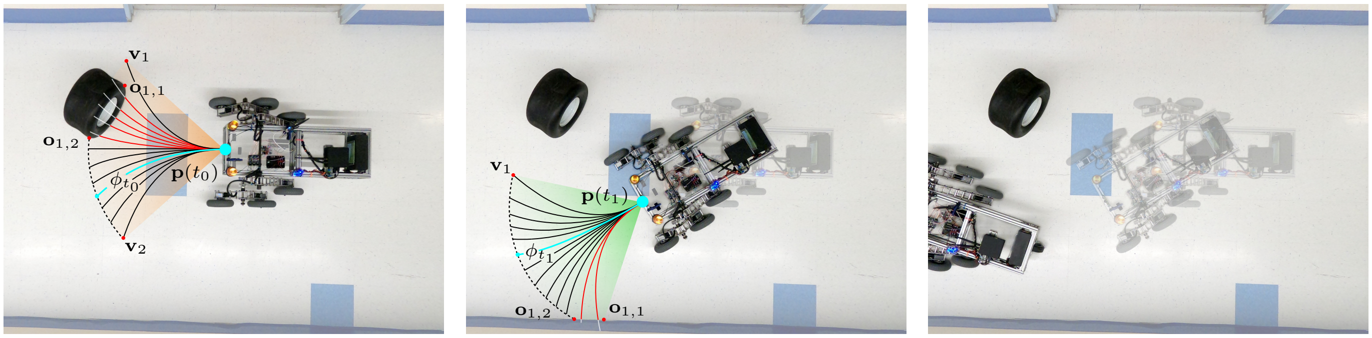

(a) . . . . (b) . . . . (c) . . . .

Fig. 2: . . . .

[47]. We propose a mixed approach for RB5 large-scale exploration framework, combining frontier- and sampling-based methods, similar to some recent approaches [44], [45], [19].

The framework evaluates local frontiers at each step, samples the environment, and determines feasible candidate path functions ϕ that intersect $\mathcal{Q}^V$ (see Definition III.1). The next ϕ is selected so that the frontier is the largest, but other costs are possible (see Sec. VI). The framework then derives a path-following vector field that points to ϕ at any point and guides the robot utilizing the gradient descent algorithm. This allows RB5 to, e.g., follow the covering path for longer and in real-time compared to approaches that utilize frontiers only, decreasing computational and cost requirements (see Sec. V).

To derive the path-following vector field, let the gradient of ϕ be defined

$$\nabla\phi := \begin{bmatrix} \partial\phi(\mathbf{p})/\mathbf{p}_x \\ \partial\phi(\mathbf{p})/\mathbf{p}_y \end{bmatrix}, \tag{1}$$

where $\partial\phi/\mathbf{p}$ is the differential, and $\mathbf{p}_x$, $\mathbf{p}_y$ are the x and y compoenents of $\mathbf{p}$. It points in the direction where ϕ maximally locally increases. To assign the direction to each point, we use the construct of vector fields, which is common in other motion planning literature [38], [40], [43]

$$\Phi(t,\phi) := \bigcup_{\mathbf{p}(t)\in\mathcal{Q}} \nabla\phi(\mathbf{p}(t)). \tag{2}$$

We modify the vector field in Equation (2) to point to the contour of the path function ϕ rather than its local maxima

$$\Delta\phi(\mathbf{p}(t)) := E\nabla\phi(\mathbf{p}(t)) - k_e\phi(\mathbf{p}(t))\nabla\phi(\mathbf{p}(t)), \tag{3}$$

where $E\nabla\phi$ points perpendicularly to the gradient and $\phi\nabla\phi$ to ϕ at $k_e \in \mathbb{R}_{>0}$ rate [40]. E is the following direction, i.e.,

$$E = \begin{bmatrix} 1 & 0 \\ 0 & -1 \end{bmatrix}, \tag{4}$$

is counterclockwise and $-E$ clockwise directions [41].

Let thus the path-following equivalent of Eq. (2) be

$$\Phi_\phi(t,\phi) := \bigcup_{\mathbf{p}(t)\in\mathcal{Q}} \Delta\phi(\mathbf{p}(t)). \tag{5}$$

The path-following vector field is summarized in the pseudo-code in Algorithm 1, with the gradient descent in Line 13. The vector $\varphi \in \mathbb{R}^2$ points RB5 in the direction of the path function ϕ with a scalar step size $\theta \in \mathbb{R}_{>0}$. The algorithm runs at the highest frequency $\mathcal{T} := \{t_0, t_0+h, \dots\}$

Algorithm 1 Derivation of the exploration coverage $\langle\phi, t\rangle$

1: **for all** $t \in \mathcal{T}$ **do**
2: **if** $\mathcal{P} \cap \mathcal{Q} = \{\varnothing\}$ **then return** $\langle\phi, t\rangle$
3: $\mathcal{Q}_t^V := O_{1,t}, O_{2,t}, \dots, O_{n,t}, V_t \leftarrow$ sensor readings
4: **if** $\mathcal{Q}_t^V \neq \mathcal{Q}_{t-1}^V$ **then**
5: $\{\phi_{1,t}, \phi_{2,t}, \dots\} \leftarrow \phi$s in Def. III.1, inters. $\mathcal{Q}^V \cap \Psi(\mathcal{Q}_t^V)$
6: **if** $\phi_t := \{\phi_{1,t}, \phi_{2,t}, \dots\} = \{\varnothing\}$ **then** RB5 is stuck
7: **else**
8: $\phi_t \leftarrow \arg\max_\phi l(\phi_t, t, \mathcal{Q}_t^V)$ in Eq. (7)
9: $\langle\phi, t\rangle \leftarrow \langle\phi, t\rangle \cup \langle\phi_t, t\rangle$ in Def. III.2
10: $\mathcal{P} \leftarrow \mathcal{P} \cup \Psi(\mathcal{Q}_t^V)$
11: **end if**
12: **end if**
13: $\varphi(t, \mathbf{p}(t)) \leftarrow \varphi(t-1, \mathbf{p}(t-1)) + \theta\Delta\phi(\mathbf{p}(t))$ in Eq. (3)
14: **end for**

with a time-step $h \in \mathbb{R}_{>0}$. Practically, there might be different hs at different times (see Sec. V). In Line 2, the algorithm evaluates if the bounded volume $\mathcal{Q}$ is covered utilizing the covered volume $\mathcal{P} \subseteq \mathbb{R}^3$. The latter is updated in Line 5, where the function $\Psi : \mathbb{R}^{2n} \times \mathbb{R}^2 \to \mathbb{R}^{3n} \times \mathbb{R}^3$ maps the vertices to the volume. The vertices of $\mathcal{Q}_t^V$ in Line 3 are derived from sensor readings, assuming the presence of a low-cost depth camera. The framework read the camera's point cloud, clustering the obstacles $O_{1,t}, O_{2,t}, \dots$ by checking if the distance between consecutive points in space is within a given threshold $\varepsilon \in \mathbb{R}_{>0}$ and deriving their vertices. The vertices of the space at time instant t, V_t are simply the limits of the sensor's field of view.

The remaining lines compute the feasible path functions $\{\phi_{1,t}, \phi_{2,t}, \dots\}$ by intersecting the space $\Psi(\mathcal{Q}_t^V)$ with possible candidate trajectories that have their final points laying at the edges of $\mathcal{Q}_t^V$, i.e., splines of the form

$$a(x-\mathbf{p}_x)^3 + b(x-\mathbf{p}_x)^2 + c(x-\mathbf{p}_x) + d - y = 0, \tag{6}$$

where $a, b, c \in \mathbb{R}$ are the coefficients of the spline. The best trajectory is then derived via the cost l in Line 8, utilizing the intersection of the largest frontier. For instance, if there are no obstacles, Eqs. (6–7) are such that ϕ is a line parallel to the direction of RB5. Formally

$$l := \{\|\mathbf{p}_1 - \mathbf{p}_2\| \mid \exists\, \mathbf{p}_1, \mathbf{p}_2 \in \Psi(\mathcal{Q}_t^V) \text{ s.t. } \mathbf{p}_1 \neq \mathbf{p}_2, \phi(\mathbf{p}_1 - \mathbf{p}_2) \approx 0\}, \tag{7}$$

where the condition $\phi(\mathbf{p}_1 - \mathbf{p}_2)$ is evaluated on a given $\varepsilon \in \mathbb{R}_{>0}$, i.e., $|\phi(\mathbf{p}_1 - \mathbf{p}_2)| < \varepsilon$.

Using the algorithm, the framework provides a way to explore space $\mathcal{Q}$ and avoid obstacles $\mathcal{Q}^{O_i}$. There are configurations at which there are no feasible trajectories nonetheless, e.g., if $\{\phi_{1,t}, \phi_{2,t}, \dots\} = \{\varnothing\}$ in Line 6. In this scenario, the framework allows a human to intervene via standard wireless and LoRa communication technology. RB5 can then be teleoperated on long distances–studies from the internet-of-things domain [32], [48] report a range of up to five kilometers in an urban setting–and with a relatively inexpensive hardware equipment (two LoRa bundles). The framework we propose utilizes a web interface to parse human commands into our custom communication protocol which utilizes the LoRa physical layer's payload to transfer φ's x and y components.

The algorithm is illustrated in Fig. 2. At each iteration, RB5 samples the environment and derives a set of possible candidate trajectories $\{\phi_{1,t}, \phi_{2,t}, \dots\}$. If there is no obstacle ahead, the optimal trajectory per iteration ϕ_t is a line parallel to RB5's direction of travel (see Fig. 2c). If there are obstacles, the framework selects the trajectory via the cost l, ϕ_t, which goes through the middle of the largest frontier (see Fig. 2a and 2b for respective obstacles "wheel" and "wall").

To derive a map of the environment and to keep the track of RB5 within it in Line 13, the framework uses a state-of-the-art visual SLAM algorithm from the literature [37]. RB5's location is also used to determine whether the exploration is complete in Line 2 and to asses exploration-to-cost (see Fig. **??**).

The framework is distributed under the popular open-source CC BY-NC-SA license[1]. It is composed of three distinct components. A "ground robot" ROS2 [33] package implements the communication with a base station using either the IEEE 802.11 wireless communication or long-range LoRa protocols. The package further implements the serial communication with the microcontroller implemented in Arduino and the vertices detection (see Algorithm 1). A "ground navigation" ROS package collects point clouds from an RGB-D sensor (an Intel (R) RealSense (TM) Depth Camera [49] D435) and other data from the SLAM algorithm [37] and ports them into ROS2. Finally, a "base server" implements the necessary functionality for remote human intervention. Both "ground robot" and "ground navigation" are implemented in C++ in ROS2 and ROS respectively, whereas "base station" is in PHP and JavaScript.

V. Field Experiments

VI. Conclusion and Future Directions

[1] github.com/adamseew/ytcg_ground-based

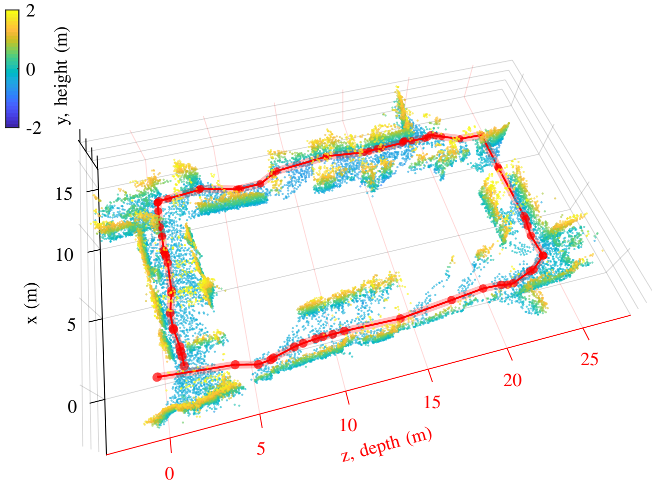

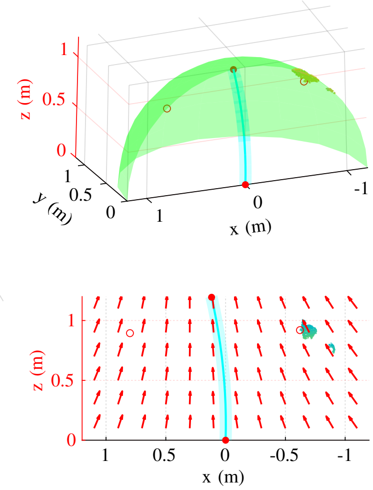

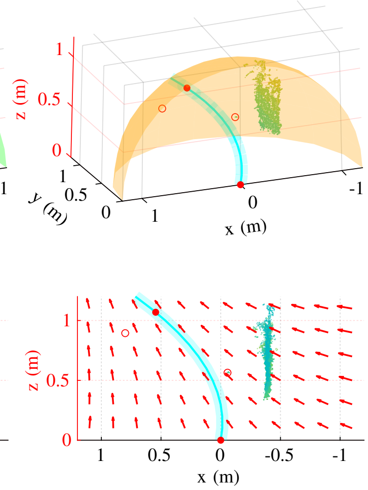

(b) . . . . (c) . . . .

(a) . . . .

Fig. 3: . . . .

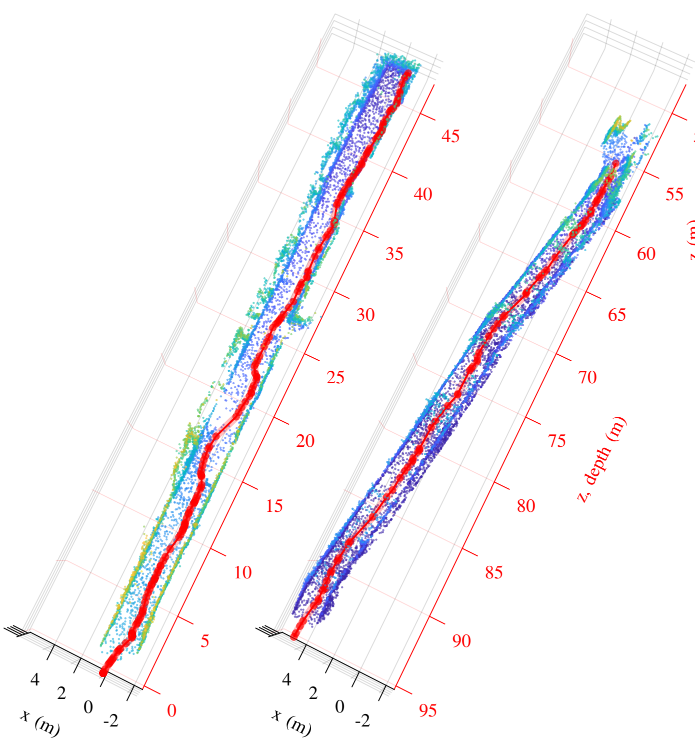

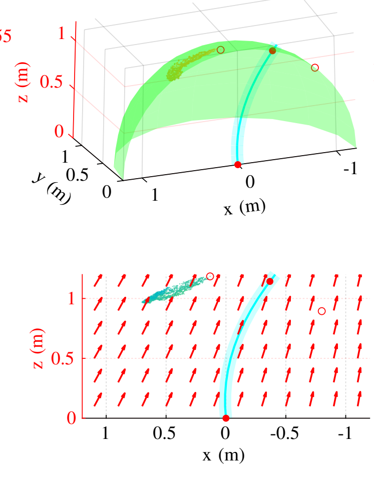

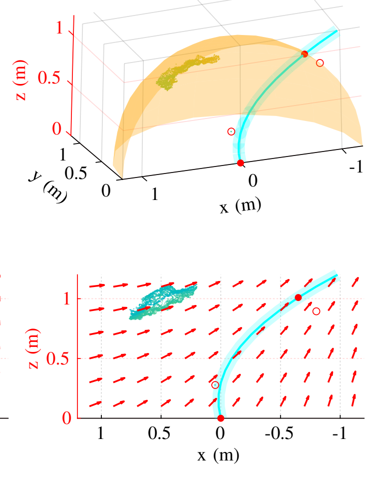

(b) . . . . (c) . . . .

(a) . . . .

Fig. 4: . . . .

References

[1] S. Kohlbrecher, J. Meyer, T. Graber *et al.*, "Hector open source modules for autonomous mapping and navigation with rescue robots," in *RoboCup 2013: Robot World Cup XVII*. Springer, pp. 624–631. 1

[2] M. Kulkarni, M. Dharmadhikari, M. Tranzatto *et al.*, "Autonomous teamed exploration of subterranean environments using legged and aerial robots," in *International Conference on Robotics and Automation (ICRA'22)*. IEEE, 2022, pp. 3306–3313. 1

[3] M. Tranzatto, F. Mascarich, L. Bernreiter *et al.*, "CERBERUS: Autonomous legged and aerial robotic exploration in the tunnel and urban circuits of the DARPA Subterranean Challenge," *Field Robotics*, vol. 2, pp. 274–324, 2022. 1

[4] H. Kim, H. Kim, S. Lee *et al.*, "Autonomous exploration in a cluttered environment for a mobile robot with 2d-map segmentation and object detection," *IEEE Robotics and Automation Letters*, vol. 7, no. 3, pp. 6343–6350, 2022. 1

[5] F. Rubio, F. Valero, and C. Llopis-Albert, "A review of mobile robots: Concepts, methods, theoretical framework, and applications," *International Journal of Advanced Robotic Systems*, vol. 16, no. 2, p. 22, 2019. 1

[6] T. Miki, J. Lee, J. Hwangbo *et al.*, "Learning robust perceptive locomotion for quadrupedal robots in the wild," *Science Robotics*, vol. 7, no. 62, p. 14, 2022. 1

[7] T. Rouček, M. Pecka, P. Čížek *et al.*, "DARPA subterranean challenge: Multi-robotic exploration of underground environments," in *Modelling and Simulation for Autonomous Systems*. Springer, 2020, pp. 274–290. 1

[8] W. Tabib, K. Goel, J. Yao *et al.*, "Autonomous cave surveying with an aerial robot," *IEEE Transactions on Robotics*, vol. 38, no. 2, pp. 1016–1032, 2022. 1, 2

[9] K. Ebadi, Y. Chang, M. Palieri *et al.*, "LAMP: Large-scale autonomous mapping and positioning for exploration of perceptually-degraded subterranean environments," in *International Conference on Robotics and Automation (ICRA'20)*. IEEE, 2020, pp. 80–86. 1, 2

[10] Y. Mei, Y.-H. Lu, C. Lee *et al.*, "Energy-efficient mobile robot exploration," in *International Conference on Robotics and Automation (ICRA'06)*. IEEE, 2006, pp. 505–511. 1

[11] R. Shrestha, F.-P. Tian, W. Feng *et al.*, "Learned map prediction for enhanced mobile robot exploration," in *International Conference on Robotics and Automation (ICRA'19)*. IEEE, 2019, pp. 1197–1204. 1

[12] A. Eldemiry, Y. Zou, Y. Li *et al.*, "Autonomous exploration of unknown indoor environments for high-quality mapping using feature-based RGB-D SLAM," *Sensors*, vol. 22, no. 14, p. 16, 2022. 1

[13] M. B. Alatise and G. P. Hancke, "A review on challenges of autonomous mobile robot and sensor fusion methods," *IEEE Access*, vol. 8, pp. 39 830–39 846, 2020. 1

[14] I. Lluvia, E. Lazkano, and A. Ansuategi, "Active mapping and robot exploration: A survey," *Sensors*, vol. 21, no. 7, 2021. 1

[15] J. A. Placed, J. Strader, H. Carrillo *et al.*, "A survey on active simultaneous localization and mapping: State of the art and new frontiers," *IEEE Transactions on Robotics*, p. 20, 2023, doi.org/10.48550/arXiv.2207.00254. 1, 2

[16] A. Bircher, M. Kamel, K. Alexis *et al.*, "Receding horizon "next-best-view" planner for 3D exploration," in *International Conference on Robotics and Automation (ICRA'16)*. IEEE, 2016, pp. 1462–1468. 1

[17] M. Müller and V. Koltun, "OpenBot: Turning smartphones into robots," in *International Conference on Robotics and Automation (ICRA'21)*. IEEE, 2021, pp. 9305–9311. 1, 2

[18] D. Tardioli, L. Riazuelo, D. Sicignano *et al.*, "Ground robotics in tunnels: Keys and lessons learned after 10 years of research and experiments," *Journal of Field Robotics*, vol. 36, no. 6, pp. 1074–1101, 2019. 1

[19] T. Dang, F. Mascarich, S. Khattak *et al.*, "Graph-based path planning for autonomous robotic exploration in subterranean environments," in *2019 IEEE/RSJ International Conference on Intelligent Robots and Systems (IROS)*. IEEE, 2019, pp. 3105–3112. 1, 2, 3

[20] H. Surmann, A. Nüchter, and J. Hertzberg, "An autonomous mobile robot with a 3D laser range finder for 3D exploration and digitalization of indoor environments," *Robotics and Autonomous Systems*, vol. 45, no. 3, pp. 181–198, 2003. 1

[21] M. Juliá, A. Gil, and O. Reinoso, "A comparison of path planning strategies for autonomous exploration and mapping of unknown environments," *Autonomous Robots*, vol. 33, pp. 427–444, 2012. 1, 2

[22] B. Yamauchi, "A frontier-based approach for autonomous exploration," in *Proceedings 1997 IEEE International Symposium on Computational Intelligence in Robotics and Automation CIRA'97. 'Towards New Computational Principles for Robotics and Automation'*, 1997, pp. 146–151. 1, 2

[23] B. Zhou, Z. Wu, and X. Liu, "Smartphone-based robot indoor localization using unertial sensors, encoder and map matching," in *International Conference on Automation, Control and Robots (ICACR'21)*. IEEE, 2021, pp. 145–149. 1

[24] S. M. F. Faisal, T. Rahman, and M. A. Kabir, "A low-cost rough terrain explorer robot fabrication using rocker bogie mechanism," in *International Conference on Computer, Communication, Chemical, Materials and Electronic Engineering (IC4ME2'21)*, 2021, pp. 1–4. 1, 2

[25] K. Ismail, R. Liu, J. Zheng *et al.*, "Mobile robot localization based on low-cost LTE and odometry in GPS-denied outdoor environment," in *International Conference on Robotics and Biomimetics (ROBIO'19)*. IEEE, 2019, pp. 2338–2343. 1

[26] "ROS-based unmanned mobile robot platform for agriculture," *Applied Sciences*, vol. 12, no. 9, p. 13, 2022. 1

[27] F. Voigtländer, A. Ramadan, J. Eichinger *et al.*, "5G for robotics: Ultra-low latency control of distributed robotic systems," in *International Symposium on Computer Science and Intelligent Controls (ISCSIC'17)*. IEEE, 2017, pp. 69–72. 1

[28] C. Delgado, L. Zanzi, X. Li *et al.*, "OROS: Orchestrating ROS-driven collaborative connected robots in mission-critical operations," in *International Symposium on a World of Wireless, Mobile and Multimedia Networks (WoWMoM'22)*. IEEE, 2022, pp. 147–156. 1

[29] C. Cadena, L. Carlone, H. Carrillo *et al.*, "Past, present, and future of simultaneous localization and mapping: Toward the robust-perception age," *IEEE Transactions on Robotics*, vol. 32, no. 6, pp. 1309–1332, 2016. 1

[30] M. Corah, C. O'Meadhra, K. Goel *et al.*, "Communication-efficient planning and mapping for multi-robot exploration in large environments," *IEEE Robotics and Automation Letters*, vol. 4, no. 2, pp. 1715–1721, 2019. 1

[31] C. Papachristos, S. Khattak, and K. Alexis, "Uncertainty-aware receding horizon exploration and mapping using aerial robots," in *International Conference on Robotics and Automation (ICRA'17)*. IEEE, 2017, pp. 4568–4575. 1

[32] J. P. Shanmuga Sundaram, W. Du, and Z. Zhao, "A survey on LoRa networking: Research problems, current solutions, and open issues," *IEEE Communications Surveys & Tutorials*, vol. 22, no. 1, pp. 371–388, 2020. 1, 4

[33] M. Quigley, K. Conley, B. Gerkey *et al.*, "ROS: An open-source robot operating system," in *ICRA Workshop on Open Source Software*, vol. 3, no. 3.2, 2009, p. 5. 2, 4

[34] T. P. Setterfield and A. Ellery, "Terrain response estimation using an instrumented rocker-bogie mobility system," *IEEE Transactions on Robotics*, vol. 29, no. 1, pp. 172–188, 2013. 2

[35] M. Mann and Z. Shiller, "Dynamic stability of a rocker bogie vehicle: Longitudinal motion," in *International Conference on Robotics and Automation (ICRA'05)*, 2005, pp. 861–866. 2

[36] D. Kim, H. Hong, H. S. Kim *et al.*, "Optimal design and kinetic analysis of a stair-climbing mobile robot with rocker-bogie mechanism," *Mechanism and Machine Theory*, vol. 50, pp. 90–108, 2012. 2

[37] M. Labbé and F. Michaud, "RTAB-Map as an open-source lidar and visual simultaneous localization and mapping library for large-scale and long-term online operation," *Journal of Field Robotics*, vol. 36, no. 2, pp. 416–446, 2019. 2, 4

[38] V. M. Goncalves, L. C. A. Pimenta, C. A. Maia *et al.*, "Vector fields for robot navigation along time-varying curves in n-dimensions," *IEEE Transactions on Robotics*, vol. 26, no. 4, pp. 647–659, 2010. 2, 3

[39] A. Seewald, H. García de Marina, H. S. Midtiby *et al.*, "Energy-aware planning-scheduling for autonomous aerial robots," in *International Conference on Intelligent Robots and Systems (IROS'22)*. IEEE, 2022, pp. 2946–2953. 2

[40] H. García de Marina, Y. A. Kapitanyuk, M. Bronz *et al.*, "Guidance algorithm for smooth trajectory tracking of a fixed wing UAV flying in wind flows," in *International Conference on Robotics and Automation (ICRA'17)*. IEEE, 2017, pp. 5740–5745. 2, 3

[41] A. Seewald, "Energy-aware coverage planning and scheduling for autonomous aerial robots," Ph.D. thesis, Syddansk Universitet, 2021, doi.org/10.21996/7ka6-r457. 2, 3

[42] D. B. Bickler, "Articulated suspension system," 1989, U.S. Patent № 4840394. 2

[43] S. M. LaValle, *Planning algorithms*. Cambridge Univ. Press, 2006. 2, 3

[44] W. Qiao, Z. Fang, and B. Si, "A sampling-based multi-tree fusion algorithm for frontier detection," *International Journal of Advanced Robotic Systems*, vol. 16, no. 4, p. 14, 2019. 2, 3

[45] A. Dai, S. Papatheodorou, N. Funk *et al.*, "Fast frontier-based information-driven autonomous exploration with an MAV," in *International Conference on Robotics and Automation (ICRA'20)*. IEEE, 2020, pp. 9570–9576. 2, 3

[46] L. Schmid, M. Pantic, R. Khanna *et al.*, "An efficient sampling-based method for online informative path planning in unknown environments," *IEEE Robotics and Automation Letters*, vol. 5, no. 2, pp. 1500–1507, 2020. 2

[47] A. Batinovic, T. Petrovic, A. Ivanovic *et al.*, "A multi-resolution frontier-based planner for autonomous 3d exploration," *IEEE Robotics and Automation Letters*, vol. 6, no. 3, pp. 4528–4535, 2021. 2

[48] U. Raza, P. Kulkarni, and M. Sooriyabandara, "Low power wide area networks: An overview," *IEEE Communications Surveys & Tutorials*, vol. 19, no. 2, pp. 855–873, 2017. 4

[49] L. Keselman, J. Iselin Woodfill, A. Grunnet-Jepsen *et al.*, "Intel RealSense stereoscopic depth cameras," in *Conference on Computer Vision and Pattern Recognition Workshops (CVPRW'17)*. IEEE, 2017, pp. 1267–1276. 4